Characteristic relationship between the maximum Josephson current and the c-axis conductivity observed for intrinsic Josephson junctions in Bi-Sr-Ca-Cu-O

AUTHOR(S):

Suzuki, M; Hamatani, T; Yamada, Y; Anagawa, K; Watanabe, T

CITATION:

Suzuki, M ...[et al]. Characteristic relationship between the maximum Josephson current and the c-axis conductivity observed for intrinsic Josephson junctions in Bi-Sr-Ca-Cu-O. IEEE TRANSACTIONS ON APPLIED SUPERCONDUCTIVITY 2005, 15(2): 189-192

ISSUE DATE:

2005-06

URL:

http://hdl.handle.net/2433/39956

Characteristic Relationship Between the Maximum Josephson Current and the c-Axis Conductivity Observed for Intrinsic Josephson Junctions in Bi-Sr-Ca-Cu-O

Minoru Suzuki, Takashi Hamatani, Yoshiharu Yamada, Kenkichi Anagawa, and Takao Watanabe

***Abstract*—The maximum Josephson current (MJC) is measured for small mesas fabricated on cleaved surfaces of $B_2Sr_2CaCu_2O_{8+\delta}$ single crystals. It is found that the MJC increases dramatically with increasing c-axis conductivity. The behavior indicates that the MJC is proportional to the square of the c-axis conductivity. This implies that the superconductivity in high-T_c superconductors is likely to be inhomogeneous.**

***Index Terms*—Bi-Sr-Ca-Cu-O, high-temperature superconductors, Josephson junctions, tunneling spectroscopy.**

I. Introduction

A puzzling property of high-T_c superconductors is the anomalous smallness of the maximum Josephson current (MJC). This has been observed for a variety of Josephson junctions made of high-T_c superconductors. The observed MJC is smaller by nearly an order of magnitude than the value expected by the Ambegaokar-Baratoff (AB) theory [1]. This may imply that the interface of a Josephson junction is imperfect and causes deterioration of the superconducting (SC) order parameter in its vicinity, which leads to the reduction of the MJC. It may also imply that the symmetry of the SC order parameter is of d-wave type [2] so that the MJC is reduced when compared with the case of s-wave symmetry. However, the relative decrease in the MJC expected in this case does not amount to $2/\pi$. A particular configuration of the order parameter at the junction interface may give rise to a very small MJC. Such a configuration is, however, very difficult to find commonly in a variety of Josephson junctions. Therefore, it is totally unknown whether the reduced MJC is caused by the degraded junction interface or by a particular configuration of the order parameters on both sides of the junction, or by an unknown origin.

Manuscript received October 4, 2004. This work was supported in part by the Mitsubishi Foundation, Iketani Science and Technology Foundation, and the 21st Century COE Program Grant of the Center of Excellence for Research and Education of Fundamental Technologies in Electrical and Electronic Engineering from Ministry of Education, Culture, Sports, Science, and Technology, Japan.

M. Suzuki, T. Hamatani, Y. Yamada, and K. Anagawa are with the Department of Electronic Science and Engineering, Kyoto University, Kyoto 615-8510, Japan (e-mail: suzuki@kuee.kyoto-u.ac.jp).

T. Watanabe is with NTT Photonics Laboratories, Nippon Telegraph and Telephone Corporation, Atsugi, Kanagawa 243-0198, Japan.

Digital Object Identifier 10.1109/TASC.2005.849747

Although the fabrication technique of the Josephson junctions has been improved [3], the quality of artificial Josephson junctions is still insufficient for the test of the theoretical model. However, intrinsic Josephson junctions (IJJ) [4], [5] observed in $B_2Sr_2CaCu_2O_{8+\delta}$ (Bi-2212) single crystals are considered to be ideal ones for this test. The tunneling barrier of the intrinsic Josephson junctions is the crystal structure itself so that there is basically no disorder or degradation in the SC order parameter. The current-voltage $(I-V)$ characteristics observed for these IJJ's exhibit deeply hysteretic tunneling behavior, which has never been observed for artificial Josephson junctions. Very small leakage current in the tunneling characteristics for these intrinsic Josephson junctions reinforced the ideal junction interface. With these ideal Josephson junctions, it becomes possible to elucidate the cause of the reduced MJC in high-T_c superconductors.

In order to observe the MJC, it is necessary to fabricate small size junctions comparable or smaller than the Josephson penetration depth λ_J, the value for which is not necessarily definite at present. According to Latyshev *et al.* [6], 20 μm is the crossover length from small junctions to large junctions. We follow their argument and fabricated junctions of the size of 10 μm square or 5 μm square. In the AB theory, the MJC is expressed as

$$J_c = \frac{\pi\Delta_{SG}}{2eR_N}\tanh\left(\frac{\Delta_{SG}}{2k_BT}\right) \simeq \frac{\pi\Delta_{SG}}{2eR_N}(k_BT \ll \Delta_{SG}), \quad (1)$$

where $2\Delta_{SG}$ is the SC order parameter or SC gap, and R_N and J_c are the normal tunneling resistance and the MJC, respectively, both across unit area. $2\Delta_{SG}$ is measured by interlayer tunneling spectroscopy [7], which makes use of IJJ's, whereas R_N is obtained from the c-axis resistivity ρ_c with a small assumption. Previous studies have shown that the theoretical prediction of the MJC density is much greater than values actually observed by more than one order of magnitude. It is found in this study that the same behavior is observed for IJJ's. Therefore, it is likely that the quality of the tunneling barrier is not a major cause of the reduced MJC in high-T_c Josephson junctions. We need to seek for a different cause other than the tunneling barrier as the origin of the reduced MJC.

In the present study aiming at a further elucidation of the origin of the reduced MJC, we varied the tunneling resistance R_N by changing the oxygen content and observed a change

in the MJC at 10 K as a function of $R_{\rm N}$. If $J_{\rm c}$ changes proportionally to $2\Delta_{\rm SG}/R_{\rm N}$, it follows that the tunneling barrier plays a dominant role in the reduced MJC. In reality, however, it is found that this is not the case but the MJC increases much more rapidly than $2\Delta_{\rm SG}/R_{\rm N}$, while $2\Delta_{\rm SG}$ decreases with the increase in $R_{\rm N}$. This behavior is totally unexpected because a decrease in $2\Delta_{\rm SG}$ usually implies a decrease in the MJC. From these considerations, it necessarily follows that this behavior is inexplicable in terms of a homogeneous superconductor. A similar behavior was observed in the $Bi_2Sr_2Ca_2Cu_3O_{10+\delta}$ system [8]. Therefore, it is highly likely that high-$T_{\rm c}$ superconductors are inhomogeneous in nature and the degree of inhomogeneity is suppressed when the doping level is increased.

II. Sample Fabrication

Small and very thin mesa structures with a square edge size of 5 or 10 μm and a typical thickness of 15 nm were fabricated on a cleaved surface of Bi-2212 single crystals grown by the traveling-solvent-floating-zone method. The mesa thickness corresponds to a stack of 10 IJJ's. The standard Ar ion milling and photolithography were employed for the mesa fabrication. Prior to the fine processing, a Au/Ag double layer was evaporated on a fresh cleaved surface. Then the crystals were annealed in an appropriate atmosphere. The carrier doping level of the samples was controlled by the annealing atmosphere and temperature. Underdoped samples were obtained by annealing in vacuum and overdoped samples were obtained in flowing oxygen at annealing temperatures ranging from 390 to 430°C for 25 to 60 min. In this way, we obtained mesa structures with ρ_c values ranging from 18 to 97 Ωcm at 300 K. The lowest SC transition temperature $T_{\rm c}$ attained was 50 K for the underdoped samples.

The sample electrode configuration is of the three-terminal type. This three-terminal configuration was adopted to provide a good heat flow channel to the upper Au electrode at the expense of the contact resistance. Nonetheless, the self-heating due to the injection of current is not negligible, especially when the doping level is high and ρ_c is small. In this case, the influence of the self-heating on the magnitude of the SC energy gap is estimated to be approximately 3% or less based on the numerical calculation and experimental analysis [9].

Values for $2\Delta_{\rm SG}$ were obtained by the short-pulse interlayer tunneling spectroscopy [7], [10]. The pulse waveform is composed of a rectangular pulse and half-wavelength sinusoidal parts placed before and after the rectangular pulse. This pulse shape was adopted to suppress puncture breakage at high applied voltages [11]. The other details were described elsewhere [11], [12].

III. Experimental Results

A. Current-Voltage $(I-V)$ Characteristics for Mesa Structures

Fig. 1 shows an oscilloscope photograph for the $I-V$ characteristics for an underdoped sample with a $T_{\rm c}$ of 60.4 K and a medium ρ_c, demonstrating resistive branches of distinct number of $N=10$, where N indicates the number of intrinsic Josephson junctions connected in series. A finite contact resistance is also seen in Fig. 1. The critical current $I_{\rm c}$, from which the MJC is evaluated, is determined from Fig. 1 to be approximately 140 μA for this sample. The value for I_c exhibits a scatter from branch to branch, and the one presumably for the outermost junction, tends to be smaller significantly than others, probably caused by possible damages during the fabrication process. Except for these smaller ones, values for $I_{\rm c}$ are nearly constant with a scatter less than 10%. The critical current density $J_{\rm c}$ is determined from $I_{\rm c}$ by dividing by the junction area actually observed with a microscope since the junction area had also a significant scatter of 0 to approximately -30%.

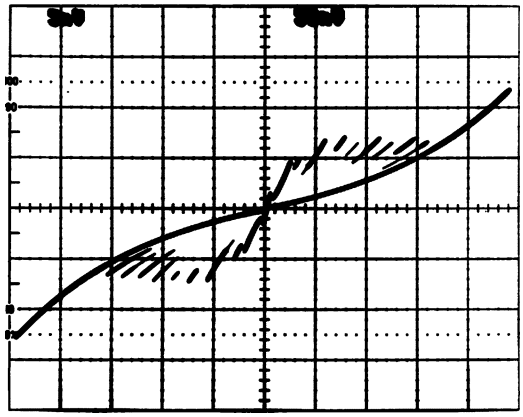

Fig. 1. Oscilloscope image of $I-V$ characteristics at 10 K for an underdoped mesa sample of $T_{\rm c}=60.3$ K. X-axis: 50 mV/div. Y-axis: 100 μA/div.

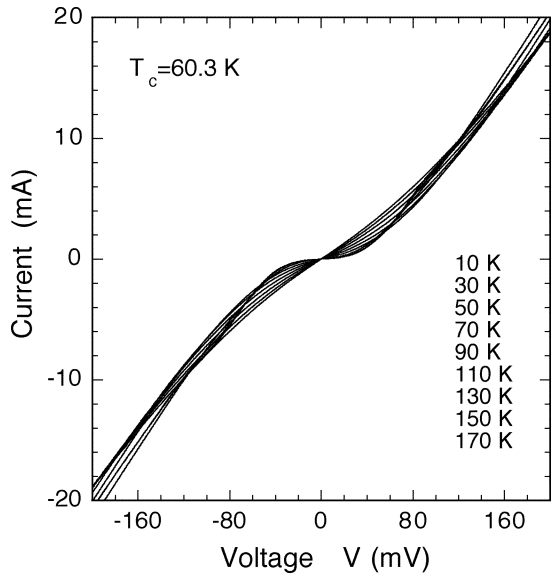

Fig. 2. $I-V$ characteristics by the short-pulse method for the sample in Fig. 1 at various temperatures. V denotes the single junction voltage.

B. Normal Tunneling Resistivity and c-Axis Resistivity

The $I-V$ characteristics by the short-pulse method is shown in Fig. 2, where the abscissa V denotes the single junction voltage. Significant extensive nonlinear curvature is seen both below and above $T_{\rm c}$. From the $I-V$ characteristics at large V, where the curves are almost linear in V, values for the normal tunneling resistance $R_{\rm N}$ are determined. In the present case, however, $R_{\rm N}$ is not necessarily immediately clear from

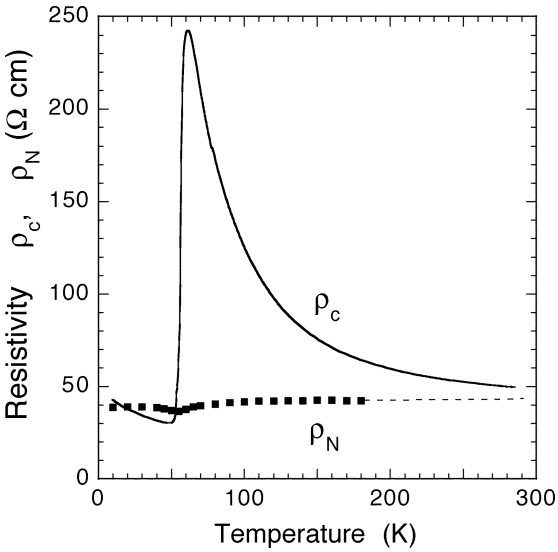

Fig. 3. Temperature dependence of ρ_c and ρ_N for the sample in Fig. 1. The dashed line indicates an extrapolation of ρ_N to 300 K.

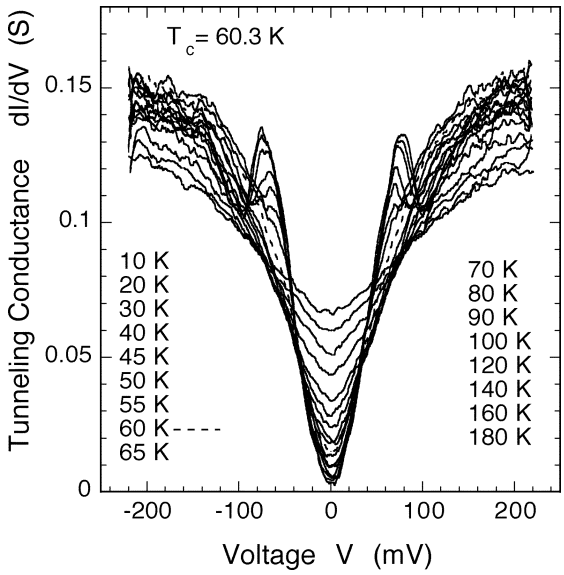

Fig. 4. $dI/dV - V$ characteristics for the sample in Fig. 1. The dashed line indicates the characteristics near T_c. V denotes the single junction voltage.

Fig. 2. Therefore, we take the value of static resistance at the highest V value in the $I-V$ curve observed. From these R_N values, we obtain values for the normal tunneling resistivity $\rho_N = R_N S/t$, where S is the mesa area and t is the mesa thickness. These ρ_N values are plotted in Fig. 3 as a function of temperature T, together with the T-dependence of c-axis resistivity (mesa resistivity) ρ_c, which was measured at a bias current of 5 μA. The thickness needed for the calculation of ρ_c was determined from the number of series connected IJJ's observed in the $I-V$ characteristics. It is seen that ρ_N is close to ρ_c at 300 K. The difference is partly due to the error involved in the determination of R_N and to the contact resistance, which is inferred to be approximately 10% at 300 K from this figure.

The T dependence of ρ_c is also shown in Fig. 3, presenting a sharp contrast to ρ_N. The semiconductive T dependence for ρ_c is due to the nonlinear $I-V$ curve due to the presence of the pseudogap and has little relevance to ρ_N.

C. Tunneling Characteristics

Fig. 4 shows a set of $dI/dV - V$ curves obtained by numerically differentiating the $I-V$ curves in Fig. 2. V denotes the single junction voltage again. Unlike the cases for optimally-doped or slightly-overdoped samples [7], the SC peak is less pronounced and the background becomes profoundly enhanced with a significant voltage and temperature dependence. This behavior is commonly seen in underdoped samples. Furthermore, the tunneling conductance dI/dV in underdoped samples exhibits a characteristic dip-and-hump structure below T_c, which is not observed for slightly overdoped samples.

The dashed line in Fig. 4 indicates the $dI/dV - V$ curve at 60 K close to T_c. Above T_c, it is seen that the tunneling conductance curve demonstrates a significant pseudogap structure. The pseudogap magnitude for the optimally doped and slightly overdoped samples is close to $2\Delta_{SG}$ [10]. In the present study, the pseudogap for this underdoped sample is found to be approximately 200 meV or higher.

The superconducting gap magnitude $2\Delta_{SG}/e$ is determined from these characteristics to be 78 mV as half the peak separation at 10 K. Values of $2\Delta_{SG}/e$ for samples with different doping levels are plotted in Fig. 5 as a function of σ_c. It is clearly seen that $2\Delta_{SG}/e$ tends to decrease as σ_c increases. The implication of plotting against σ_c is explained in the next section.

D. Maximum Josephson Current

Values of the MJC density J_c for samples with different doping levels are plotted as a function of σ_c in Fig. 5. As suggested earlier [12], [13], J_c increases rapidly as σ_c increases. In particular, for a sample with $\sigma_c > 0.05$ S cm^{-1}, J_c exceeds 4000 A/cm^2, an order of magnitude larger than that for an underdoped sample.

IV. Discussion

A. c-Axis Conductivity as a Doping Parameter

In the preceding section, it was shown that ρ_N is nearly equal to ρ_c at 300 K. Since the electrical conduction in the c-axis direction is considered to arise via the tunneling between the CuO_2 planes, we assume that the carrier concentration is proportional to the c-axis conductivity $\sigma_c = \rho_c^{-1}$. This is based on the idea that the carrier concentration is proportional to the density of states when the dispersion is suppressed in the tunneling direction and that the tunneling conductance is proportional to the density of states. In an inhomogeneous case, like a recent model [14] proposed for high-T_c superconductors, the area of the conductive region is considered to be proportional to the carrier concentration. Therefore, it follows that σ_c is approximately proportional to the carrier concentration whether the system is described by the conventional model or newly proposed topologically inhomogeneous model. Based on this idea, we regard the c-axis conductivity as the main parameter representing the carrier concentration or carrier doping level.

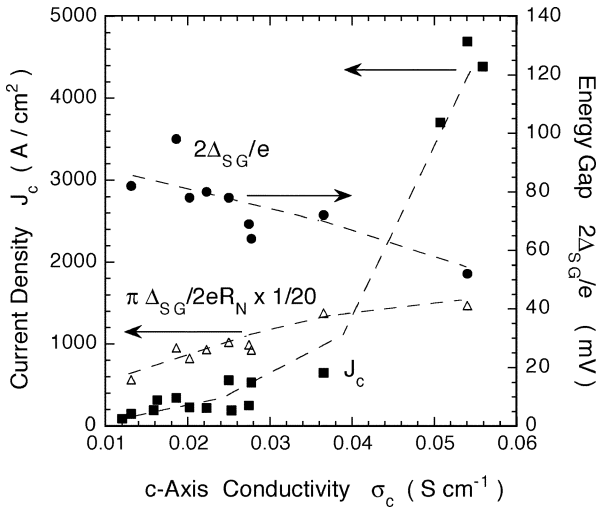

Fig. 5. MJC density J_c, the SC gap $2\Delta_{SG}$, and the theoretical MJC density obtained by using ρ_c and $2\Delta_{SG}$. The dashed lines are the guides to the eyes.

Thus, when σ_c increases, it means that the carrier doping level is increased. In this sense, Fig. 5 indicates the doping dependence of J_c and $2\Delta_{SG}/e$. In the present study, ρ_c decreases from 97 to 18 Ωcm, which implies σ_c increases from 0.01 to 0.056 S cm^{-1}, as the carrier doping level increases. This change in σ_c corresponds to the change in the hole density p from $p = 0.09$ to 0.18.

B. Characteristic Relationship Between J_c and σ_c

Using the values obtained for ρ_c and $2\Delta_{SG}/e$, we calculated the low temperature MJC, i.e., $\pi\Delta_{SG}/2eR_N$ using (1). The results are plotted in Fig. 5. It is clearly seen that the observed J_c is approximately one order of magnitude smaller than the AB theory. Furthermore, J_c increases much more rapidly than the tendency expected by the AB theory. This behavior cannot be explained in terms of the usual concept of homogeneous superconductors, but is likely to be explicable only by invoking the concept of inhomogeneous superconductivity.

In the present model, CuO_2 sheets are considered to be inhomogeneous and composed of SC and nonsuperconducting regions on a very fine scale. Let f be the fraction of the SC area. Then f is proportional to the carrier concentration, so that it approximately follows that $f \propto \sigma_c$. In the present model, it is very important that the Josephson current flows only in the local area where both sides of the IJJ barrier are superconducting. Therefore, it is simply conjectured that the Josephson current is proportional to f^2 rather than f, i.e., $J_c \propto f^2$. Then it follows that $J_c \propto \sigma_c^2$. This relationship should be compared with the experimental result shown in Fig. 5. Clearly, the experimental data shows a strong tendency to obey this relationship. This indicates that the SC state in high-T_c superconductors is likely to be inhomogeneous in its nature. This inhomogeneous nature appears to diminish when the doping level increases because the fraction f increases. Therefore, overdoped superconductors are expected to exhibit normal SC behavior like conventional superconductors. This is actually the case for the tunneling spectroscopy results [10].

The experimental data for MJC in IJJ's has shown that $J_c \propto \sigma_c^2$. From this relationship we obtain $J_c\rho_N \propto \sigma_c$, and finally $J_c\rho_N \propto J_c^{1/2}$, which is commonly observed for artificial Josephson junctions [15]. Thus the characteristic relationship between MJC and σ_c is likely to be essential in high-T_c superconductors.

V. Conclusion

The maximum Josephson current density J_c and the SC gap are measured for small mesas fabricated on cleaved surfaces of $Bi_2Sr_2CaCu_2O_{8+\delta}$ single crystals with various carrier doing levels and c-axis conductivities. It is found that J_c increases dramatically with increasing c-axis conductivity. The behavior indicates that J_c is proportional to the square of the c-axis conductivity. This implies that the superconductivity in high-T_c superconductors is likely to be inhomogeneous.

References

[1] V. Ambegaokar and A. Baratoff, "Tunneling between superconductors," *Phys. Rev. Lett.*, vol. 10, no. 11, pp. 486–489, Jun. 1963.
[2] C. C. Tsuei and J. R. Kirtley, "Pairing symmetry in cuprate superconductors," *Rev. Mod. Phys.*, vol. 72, no. 4, pp. 969–1016, Oct. 2000.
[3] K. Kuroda, Y. Wada, T. Takami, and T. Ozeki, "Fabrication of full high-T_c superconducting $YBa_2Cu_3O_{7-x}$ trilayer junctions using a polishing technique," *Jpn. J. Appl. Phys.*, pt. 2, vol. 42, no. 8B, pp. L1006–L1008, Aug. 2003.
[4] R. Kleiner, F. Steinmeyer, G. Kunkel, and P. Müller, "Intrinsic Josephson effects in $Bi_2Sr_2CaCu_2O_8$ single crystals," *Phys. Rev. Lett.*, vol. 68, no. 15, pp. 2394–2397, Apr. 1992.
[5] A. A. Yurgens, "Intrinsic Josephson junctions: recent developments," *Supercond. Sci. Technol.*, vol. 13, no. 8, pp. R85–R100, Aug. 2000.
[6] Y. I. Latyshev, J. E. Nevelskaya, and P. Monceau, "Dimensional crossover for intrinsic dc Josephson effect in $Bi_2Sr_2CaCu_2O_8$ 2212 single crystal whiskers," *Phys. Rev. Lett.*, vol. 77, no. 5, pp. 932–935, Jul. 1996.
[7] M. Suzuki, A. Matsuda, and T. Watanabe, "Interlayer tunneling spectroscopy for slightly overdoped $Bi_2Sr_2CaCu_2O_{8+\delta}$," *Phys. Rev. Lett.*, vol. 86, no. 26, pp. 5361–5364, June 1999.
[8] Y. Yamada, K. Anagawa, T. Shibauchi, T. Fujii, T. Watanabe, A. Matsuda, and M. Suzuki, "Interlayer tunneling spectroscopy and doping-dependent energy-gap structure of the trilayer superconductor $Bi_2Sr_2Ca_2Cu_3O_{10+\delta}$," *Phys. Rev. B*, vol. 68, no. 5, pp. 054 533-1–054 533-11, Aug. 2003.
[9] K. Anagawa, Y. Yamada, T. Shibauchi, M. Suzuki, and T. Watanabe, "60 ns time scale short pulse interlayer tunneling spectroscopy for $Bi_2Sr_2CaCu_2O_{8+\delta}$," *Appl. Phys. Lett.*, vol. 83, no. 12, pp. 2381–2383, Sep. 2003.
[10] M. Suzuki and T. Watanabe, "Discriminating the superconducting gap from the pseudogap in $Bi_2Sr_2CaCu_2O_{8+\delta}$ by interlayer tunneling spectroscopy," *Phys. Rev. Lett.*, vol. 85, no. 22, pp. 4787–4790, Nov. 2000.
[11] T. Hamatani, K. Anagawa, T. Watanabe, and M. Suzuki, "Extended-range short-pulse interlayer tunneling spectroscopy for $Bi_2Sr_2CaCu_2O_{8+\delta}$ intrinsic Josephson junctions," *Physica C*, vol. 390, no. 2, pp. 89–94, Jun. 2003.
[12] M. Suzuki, T. Watanabe, and A. Matsuda, "Characteristic temperature dependence of the maximum Josephson current in Bi-Sr-Ca-Cu-O intrinsic junctions," *IEEE Trans. Appl. Supercond.*, vol. 9, no. 2, pp. 4511–4514, Jun. 1999.
[13] M. Suzuki and S. Karimoto, "Properties of intrinsic Josephson junctions in $Bi_2Sr_2CaCu_2O_{8+\delta}$ single crystals," *IEICE Trans. Electron.*, vol. E81-C, no. 10, pp. 1518–1525, Oct. 1998.
[14] S. A. Kivelson, E. Fradkin, and V. J. Emery, "Electronic liquid-crystal phases of a doped mott insulator," *Nature*, vol. 393, no. 6685, pp. 550–553, Jun. 1998.
[15] R. Gross, P. Chaudhari, M. Kawasaki, and A. Gupta, "Scaling behavior in electrical transport across grain boundaries in $YBa_2Cu_3O_{7-\delta}$ superconductors," *Phys. Rev. B*, vol. 42, no. 16, pp. 10 735–10 737, Dec. 1990.